Monitoring antiferromagnetism via angle-resolved Auger photoelectron coincidence spectroscopy: The case of NiO/Ag(001)

R. Gotter,[1] M. Sbroscia,[2] M. Caminale,[3,*] S. R. Vaidya,[1,4] E. Perfetto,[5] R. Moroni,[6] F. Bisio,[6] S. Iacobucci,[7] G. Di Filippo,[2] F. Offi,[8] A. Ruocco,[8] G. Stefani,[8] L. Mattera,[3] and M. Cini[5,9]

[1]*CNR-IOM, Istituto Officina dei Materiali, c/o Area Science Park, SS 14 Km 163.5, I-34149 Basovizza, Trieste, Italy*

[2]*Scuola Dottorale in Matematica e Fisica, Università degli Studi Roma Tre, Via della Vasca Navale 84, I-00146 Roma, Italy*

[3]*Dipartimento di Fisica, Università degli Studi di Genova, via Dodecaneso 33, I-16146 Genova, Italy*

[4]*Scuola di Dottorato in Nanotecnologie, Università degli Studi di Trieste, Piazzale Europa 1, I-34127 Trieste, Italy*

[5]*Dipartimento di Fisica, Università degli Studi di Roma Tor Vergata, Via della Ricerca Scientifica 1, I-00133 Roma, Italy*

[6]*CNR-SPIN, Istituto superconduttori, materiali innovativi e dispositivi, Sezione di Genova, Corso Perrone 24, I-16152 Genova, Italy*

[7]*CNR-IFN, Istituto Fotonica e Nanotecnologie, c/o Dipartimento di Scienze, Università degli Studi Roma Tre, Via della Vasca Navale 84, I-00146 Roma, Italy*

[8]*Dipartimento di Scienze e Unità CNISM, Università degli Studi Roma Tre, Via della Vasca Navale 84, I-00146 Roma, Italy*

[9]*Laboratori Nazionali di Frascati, Istituto Nazionale di Fisica Nucleare, Via Enrico Fermi 40, I-00044 Frascati, Roma, Italy*

(Received 3 July 2013; published 4 September 2013)

Spin selectivity in angle-resolved Auger photoelectron coincidence spectroscopy (AR-APECS) is used to probe electronic structure in antiferromagnetic thin films. In particular, exploiting the AR-APECS capability to discriminate Auger electron emission events characterized by a different spin of the ion in its final state, a sharp multiplet structure in the Ni *MVV* Auger line shape of NiO/Ag(001) thin films is measured below the critical Néel temperature. The assignment of multiplet terms follows from a close comparison of the experimental AR-APECS line shapes with the predictions based on *semiempirical* calculations on a cluster model and an open-band extension of the Cini-Sawatzky approach. In analogy to CoO, also in NiO, above the Néel temperature a more featureless Auger spectrum appears and AR-APECS does not disentangle anymore high-spin and low-spin contributions to the total Auger intensity. Such a behavior, which seems to be a general result for metal oxide antiferromagnetic systems, is discussed.

DOI: 10.1103/PhysRevB.88.094403 PACS number(s): 75.70.−i, 71.10.−w, 82.80.Pv, 79.60.Dp

A fundamental issue in magnetism is the origin of the magnetic properties at the atomic level, or, in other words, the investigation of the changes in the electronic and magnetic structure around a single atom in a solid crossing the magnetic transition temperature.

It is common knowledge that for magnetic materials at temperatures well below the transition temperature, exchange splitting separates the valence band in two pure spin states (majority vs minority spin bands) and that long-range magnetic order, be that a ferro- (FM) or antiferro- (AFM) magnetic one, is established throughout the solid.[1,2] What happens to the magnetic properties, to the local ones in particular, upon crossing the magnetic transition temperature is still a relevant and highly debated issue. It is well established that increasing the temperature, the magnetization is lowered until the long-range magnetic order is lost upon reaching the phase transition temperature. Whether exchange splitting suffers an equally drastic collapse or local magnetization randomizes while magnetic moment is preserved at the atomic level, is still an open question in this respect. There are several conflicting experimental evidences. In FM, for instance, neutron and electron scattering experiments point to the existence of local magnetic moments above the Curie temperature,[3,4] while photoemission, inverse photoemission, and scanning tunneling microscopy give conflicting pictures of collapsing exchange splitting, spin-mixing or intermediate band behavior (see, for example, Ref. 5, and references therein).

The issue of local magnetic order is even more complex in the case of AFM materials, where the magnetic moments change direction on the length scale of first neighbor atomic distances and few techniques are available for the investigation of magnetic properties (x-ray magnetic linear dichroism is one of the few examples). The ordering temperature of AFM thin films has been often inferred by monitoring the change in the magnetic properties of an adjacent FM film.[6] Such estimations can be influenced by the magnetic interaction at the interface and may not be representative of the Néel temperature (T_N) of the investigated antiferromagnet.[7] However, recent experiments[8] and theories[9] support the claim that, in AFM transition-metal oxides, atomic magnetic moments are nonzero well above T_N.

It is very interesting, therefore, to investigate the local change in electronic structure when the temperature of the magnetic transition is crossed. The ability to probe and describe itinerant electrons is of crucial relevance in order to understand the basic mechanism that leads to correlation and magnetism in solids. From the theoretical viewpoint, spin-polarized density functional theory (DFT) calculations are the basis for determining magnetic moments and can also be used to highlight the basic mechanisms governing magnetism in solids. While experimental methods sensitive to both local magnetic moments and correlation energies are highly desirable, the discrimination power of most electronic-structural spectroscopies is indeed limited by the requirement of long-range order to achieve magnetic or spin contrast, order which is lost above the critical temperature. Few methods have been developed to meet the request for a spectroscopy sensitive to local changes in magnetization, as, for example,

spin-resolved resonant photoemission,[5] spin-dependent two-photon photoemission.[10] and muon spin rotation.[11] Nonetheless, questions are still open and by this paper we shall contribute to the subject with the results of a combined experimental and theoretical effort that joins locality of the core level photoemission with sensitivity to valence band correlation of Core-Valence-Valence (CVV) Auger decays. The method consists in the core level photoionization and in the time-correlated[12] as well as angle-correlated[13,14] detection of the resulting Auger-photoelectron pair. In this way spin sensitivity and access to the spin state of the two valence holes in the system is achieved, without the need to detect the spin of the emitted electron pair.[15] The dichroic effect recently discovered in Auger-photoelectron coincidence spectroscopy (APECS) has been demonstrated as a suitable tool to study Auger line shapes in complex systems such as magnetic thin films and multilayers.[16] This peculiar property of angle-resolved (AR)-APECS, first suggested by experiments on nonmagnetic materials,[15] has been successfully applied for investigating FM as well as AFM thin films. In one case, in order to interpret the aforementioned dichroic effect including a proper theoretical description of angle-dependent Auger spectra, the Fe/Cu(001) was investigated in the FM state.[17] In this experiment the authors found that, while contributions to the spectrum from decay channels that involve minority-spin electrons are well described within an independent electron approximation, significant correlation effects must be included to account for the final state with two majority-spin holes. In another case the AFM CoO/Ag(001) surface was examined, taking measurements above and below the Néel temperature (T_N) of the compound. The sharp change observed upon crossing T_N, dubbed dichroic effect in angle-resolved (DEAR)-APECS, provided a way to probe concomitant changes in the short-range magnetic order.[18] Furthermore, the high- and low-spin contributions to the Auger spectrum were told apart and the most prominent features of the spectrum were assigned.[19] The crucial point was that the DEAR-APECS effect, able to discriminate among multiplet structures having different spin, was present below T_N and completely disappeared above T_N. In order to understand whether the CoO case is an exception or the disappearance of the dichroic effect upon crossing the antiferromagnetic-paramagnetic transition is a more general effect, we investigate in the present paper the NiO/Ag(001). A full description of the theory used to ascribe the multiplet terms contribution to the Auger intensity also will be given. The paper is organized as follows: Sec. I introduces the experimental and theoretical methods. The results of measurements and simulations are presented in Sec. II and discussed in Sec. III. Finally, Sec. IV is devoted to conclusions.

I. METHODS

A. Experiments

The experiments reported in this paper were carried out at the ALOISA beamline of the ELETTRA synchrotron radiation facility (Basovizza, Trieste, Italy). They have been performed at room temperature and 420 K, without any prior magnetic treatment of the NiO films grown on Ag(001). The Ag(001) substrate was cleaned in the vacuum chamber by 1-keV Ar^+-ion sputtering and subsequently annealed up to about 750 K. The presence of contaminants on the substrate surface was checked to be below the detection limit in x-ray photoemission spectra, while the surface crystalline order has been checked by reflection high-energy electron diffraction. NiO films have been grown on Ag(001) by reactive deposition of Ni in O_2 atmosphere. Ni was evaporated at a rate of about 0.2 Å/min in an O_2 atmosphere at a pressure of 1×10^{-7} hPa. After the evaporation the film was annealed at 540 K in an O_2 pressure of 1×10^{-6} hPa. This procedure is known to lead to the formation of NiO(001) films while preventing the embedding of metallic Ni clusters in the Ag substrate.[20,21] Film thickness was monitored by calibrating the evaporation rate with a quartz-crystal microbalance and by *a posteriori* thickness estimations using photoemission intensity of O-1*s* and Ag-3*d*.[22] The thickness of the films used in subsequent measurements has been estimated to be 15 ± 5 Å, corresponding to 7.5 ± 2.5 monolayers.

NiO films grown on Ag(001) are antiferromagnetically ordered with a T_N which depends on the NiO film thickness and a domain structure which favors those with the main spin component aligned with the film plane.[23] X-ray magnetic linear dichroism at the Ni-$L_{2,3}$ edge has been used to assess the magnetic structure and its temperature dependence in NiO films grown on different substrates and for different coverages.[23–26] In the case of NiO films grown on MgO(001) and Ag(001) substrates, it was found that the magnetic phase change can be detected from the temperature dependence of the ratio of the intensities of the two main peaks in the Ni-L_2 edge measured for linearly polarized x rays with polarization perpendicular to the main spin projection.[23,24] In Fig. 1, the absorption spectra around the Ni-L_2 edge at three different temperatures for a 15-Å-thick film are shown. The absorption spectra have been measured with linearly polarized x rays with the electric field vector forming an angle of 6° with the surface normal (x-ray polarization perpendicular to the main spin projection). The spectra, after the subtraction of a linear background, have been normalized to unity at the low-energy peak to show the redistribution of intensity for the main components of the edge as a function of temperature. In Fig. 2, the Ni-L_2 peak-intensity ratio for a 15-Å-thick

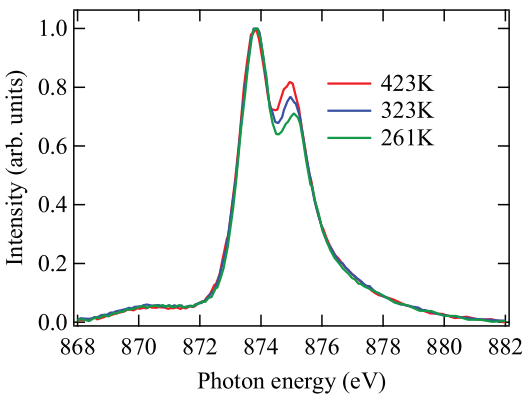

FIG. 1. (Color online) Ni-L_2 absorption edge at three different temperatures for a 15-Å-thick film after a linear background subtraction. Normalization to unity for the low-energy peak is performed to show changes in relative intensity of the two main components of the edge.

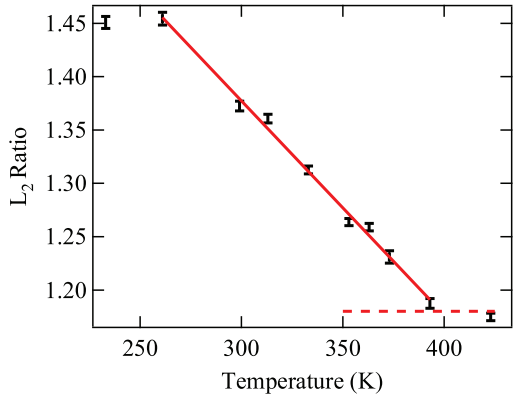

FIG. 2. (Color online) Intensity ratio of the two main components of Ni-L_2 absorption edge acquired at different sample temperatures (for the geometry, see text). The lines are a guide for the eyes.

NiO film is shown as a function of the temperature. In agreement with Ref. 24, the data show a decrease of the Ni-L_2 peak-intensity ratio for increasing T up to the reaching of a steady value above 390 K in correspondence to the crossing of T_N. Hence, AR-APECS measurements have been performed at two temperatures that are definitively above and below T_N.

The AR-APECS experimental setup is discussed in detail elsewhere.[27] Monochromatic, linearly polarized photons of 250 eV energy impinged on the sample at grazing incidence of about 6°, with the sample normal in the plane defined by $\vec{\epsilon}$, the light polarization, and $\vec{k}$, its propagation vector. The experimental chamber hosts six hemispherical electron analyzers. Out of the six electron analyzers, five were set to detect Ni $3p$ core level photoelectrons within an energy window of 4.3 eV, fixed by the analyzer energy resolution, suitable for collecting the entire Ni $3p$ main peak. They were positioned onto the plane defined by $\vec{\epsilon}$ and $\vec{k}$, at different polar angles with respect to $\vec{\epsilon}$: One was aligned with $\vec{\epsilon}$, two were $\pm 18°$ apart from it, and the other two were $\pm 36°$ apart from it. The sixth electron analyzer was devoted to measure (Ni $M_{23}M_{45}M_{45}$) Auger electrons analyzing the kinetic energies by means of a multichannel acquisition system based on multichannel plate detectors coupled with a two-dimensional delay line anode. It was positioned 38° apart from $\vec{\epsilon}$, in the plane containing $\vec{\epsilon}$ and perpendicular to $\vec{k}$. The description of the dichroism effect in AR-APECS achieving a spin selectivity in the final Auger state has been already discussed in previous papers.[13,15,28] Only a brief description of the effect is given here: The three photoelectron analyzers positioned at a relatively small (less than 20°) angular separation with respect to $\vec{\epsilon}$, collect dominant contribution from partial waves having $m = 0$ of the emitted photocurrent. The remaining two of five photoelectron analyzers, positioned 36° away with respect to $\vec{\epsilon}$, detect instead a sizable amount of $m = \pm 1$ components of the emitted photoelectrons. Analogously, the Auger analyzer, at 38° from $\vec{\epsilon}$, collects a sizable amount of partial waves having $|m| > 0$ of the emitted Auger current. We will refer to as aligned (A) for analyzers collecting dominant contributions from partial waves having $m = 0$ of the emitted electrons, and not aligned (N) for analyzers collecting a sizable contribution from those with $m > 0$. Therefore, depending upon the different angular positions of the five photoelectron analyzers there are two possible ways to combine coincident photoelectron and Auger electron pairs; AN geometry (photoelectron analyzers aligned and auger electron analyzer not aligned) and NN geometry (both photoelectron analyzer and Auger electron analyzer not aligned). Based on selection rules governing the photoemission and the Auger decay and taking into account the matrix elements connecting initial and final states, several combinations of the photoelectron and Auger electron m values combine into multiplet terms of the Auger final state, which are characterized by different values of the total spin. By choosing geometries which combine different directions of the two emitted electrons, thus weighting in a different way their m partial waves, a spin selectivity is achieved.[15]

B. Theoretical approach

The Cini-Sawatzky approach[29,30] explains how correlation effects tune the occurrence of bandlike versus atomiclike Auger core-valence-valence spectra, but is intended for closed shell spectra and does not apply to metallic bands. For decades, little information has been gained from open-band spectra, since the data themselves discourage the investigation. Indeed, core-valence-valence Auger spectra from metals like Cr, Fe, and Co and compounds like CoO resulted to be too smooth and featureless to raise much interest. In particular, they seemed to have a bandlike appearance, even if the magnetism hints at quite strong correlations. Drchal and one of us[31] proposed a theory in which some spectral features are *unrelaxed*, that is, arise from the propagation of two holes in an unpolarized rigid background, similar to the closed-bands case; the *relaxed* part of the spectrum comes from a screened state and involves the screening cloud. This can be considered as a simplified version of the more complete but demanding Gunnarsson-Schönhammer theory.[32] In this work, motivated by the APECS data, we adopt the view of Ref. 31, assuming that the Auger transition occurs when the valence band is in its ground state. Finally we point out that this case study has general implications on electron spectroscopy and also in the field of magnetism.

To describe the band states, we set up a model, which is suitable for transition metal oxides, where the NiO crystal is modeled by an octahedral NiO_6 cluster centered on the cation and parametrized for NiO. The model includes the O $2p$–Ni $3d$ hybridization and the d-d Coulomb repulsion between holes located at the Ni site, which will be treated by means of exact diagonalization. Then, we show how by a combination of theoretical and experimental techniques one can reveal considerable structure in the Auger data, and interpret it in terms of the spin selectivity of APECS. We include a minimal basis set and parameters are chosen by comparing the one-particle local density of states (LDOS) of the cluster ground state with two holes to the experimental XPS profile; the Auger spectrum is then calculated without any adjustable parameter. We recall that a similar model has been employed in previous works by Fujimori and Minami,[33] and by Zaanen, Sawatzky and Allen[35] to calculate the XPS spectrum of NiO, but only a reduced set of many-hole states was considered. In the present work we, instead, compute the 2,3,4-hole spectra of the cluster by performing the full many-particle configuration interaction corresponding to the one-particle basis set described below.

The linear combinations of $3d$ orbitals which form the e_g and t_{2g} irreducible representations (irreps) of the octahedral group are a suitable one-particle basis for the Ni ion. We take into account only the combinations of $2p$ orbitals with symmetry e_g and t_{2g},

$$p_{\Gamma\gamma} = \sum_{\substack{J \\ j=x,y,z}} c_{Jj}^{\Gamma\gamma}\, p_{Jj}, \tag{1}$$

where J runs over the six oxygens, Γ runs over the irreps, and γ over the corresponding components. In this basis the noninteracting part of the Hamiltonian reads

$$H_0 = \sum_{\Gamma=e_g,t_{2g}} \sum_{\gamma} [\epsilon_d(\Gamma) d_{\Gamma\gamma}^{\dagger} d_{\Gamma\gamma} + \epsilon_p(\Gamma) p_{\Gamma\gamma}^{\dagger} p_{\Gamma\gamma} + t_{pd}(\Gamma,\gamma)(d_{\Gamma\gamma}^{\dagger} p_{\Gamma\gamma} + p_{\Gamma\gamma}^{\dagger} d_{\Gamma\gamma})], \tag{2}$$

where the hopping parameters are the following linear combinations of Slater-Koster matrix elements[36] $E_{\Gamma\gamma,j}(J)$:

$$t_{pd}(\Gamma,\gamma) = \sum_{\substack{J \\ j=x,y,z}} c_{Jj}^{\Gamma\gamma} E_{\Gamma\gamma,j}(J). \tag{3}$$

In the above equation the oxygen J is specified by the direction cosines (l,m,n) and the energies $E_{\Gamma\gamma,j}(J)$ are expressed in terms of τ_σ and τ_π transfer integrals. As in previous works[33,35] we include the on-site repulsion in the Ni ion and neglect it on the O sites. The interaction part of the Hamiltonian is taken in the standard form:

$$H_{\text{int}} = \sum_{mm'nn'} \sum_{\sigma\sigma'} U_{mm'nn'} d_{m\sigma}^{\dagger} d_{m'\sigma'}^{\dagger} d_{n'\sigma'} d_{n\sigma}, \tag{4}$$

where the m,m',n,n' run over the Ni orbitals; the $U_{mm'nn'}$ elements can be written in terms of Slater integrals which, in turn, are expressed in terms of the Racah parameters[37] A, B, C according to $f^4 = \frac{63}{5}C$, $f^0 = A + \frac{1}{9}f^4$, $f^2 = \frac{441}{9}B + \frac{5}{9}f^4$. As only A is affected by the solid-state screening we use $B = 0.13$ eV and $C = 0.63$ eV like in the isolated Ni.[37] Eventually by a unitary transformation we rewrite H_{int} in the symmetry adapted basis (Γ,γ). In the nonrelativistic limit we write the perturbation causing the Meitner-Auger decay,

$$H_{\text{MA}} = \sum T_A c_{2p\sigma}^{\dagger} c_{k\sigma'}^{\dagger} + \text{H.c.}, \tag{5}$$

where $c_{2p\sigma}^{\dagger}$ creates the core electron, $c_{k\sigma'}^{\dagger}$ creates the Auger electron, and using an obvious notation the final-state valence holes are created by

$$T_A = \sum_{m_1,m_2} M(m_{\text{core}}, \overrightarrow{k}, m_1, m_2) c_{m_1,\sigma} c_{m_2,\sigma'}. \tag{6}$$

The Auger matrix elements are

$$M(m_{\text{core}}, \overrightarrow{k}, m_1, m_2) = \left\langle \psi_{2pm_{\text{core}}}(1) \psi_{\overrightarrow{k}}(2) \left| \frac{1}{r_{12}} \right| \psi_{2pm_{\text{core}}}(1) \psi_{\overrightarrow{k}}(2) \right\rangle. \tag{7}$$

To deal with the Auger line shape we assumed that the unrelaxed limit is appropriate. Therefore as in Ref. 19 we started by solving

$$H|\Psi_{gs,\text{Hund}}\rangle = E_{gs}|\Psi_{gs,\text{Hund}}\rangle \tag{8}$$

Here $|\Psi_{gs,\text{Hund}}\rangle$ denotes the state with the lowest energy in the maximum spin sector, namely, $S_{gs} = 1$ is the spin assumed for the Ni (d^8 configuration), like previously we used $S_{gs} = \frac{3}{2}$ for the Co (d^7 configuration).[19]

Up to a proportionality constant, the Auger spectrum is taken to be

$$J(\omega) = \sum_{\sigma'} \langle \Psi_{gs,\text{Hund}} | T_A^{\dagger} \delta(\omega - H) T_A | \Psi_{gs,\text{Hund}} \rangle, \tag{9}$$

fixing the spin quantization direction with $\sigma = \frac{1}{2}$. The exchange matrix element is understood for $\sigma = \sigma'$. In this way we considered for simplicity only the diagonal contributions (the hole states created by T_A are the same as those annihilated by $T_A^{\dagger}$) since they are the most important. We also need to resolve the Auger spectrum according to the total spin of the final states. Accordingly, we define

$$W(a,b,\sigma') = \begin{cases} |M(a,b)|^2, & \sigma' = -\frac{1}{2} \\ |M(a,b) - M(b,a)|^2, & \sigma' = \frac{1}{2}, \end{cases} \tag{10}$$

where $M(a,b) = M(m_{\text{core}}, \overrightarrow{k}, a, b)$. Then, we write

$$J_A = \sum_{S,M_S,\sigma'} \sum_{a,b}^{5} \delta(\sigma + \sigma' + S_{gs}, M_S) \times W(a,b,\sigma') \rho(a,b,S,\sigma,\sigma'), \tag{11}$$

where

$$\rho(a,b,S,\sigma,\sigma') = \langle d^8 S_z = S_{gs} | c_{b\sigma'} c_{a\sigma} \delta(\omega - H) \times P^S c_{a\sigma}^{\dagger} c_{b\sigma'}^{\dagger} | d^8 S_z = S_{gs} \rangle, \tag{12}$$

and P^S is the operator which projects on the total spin S.

We computed the $M_{ck\alpha\beta}$ matrix elements for the $M_{23}M_{45}M_{45}$ transitions using the Clementi-Roetti atomic orbitals[34] for positive ions and plane waves for the Auger electrons; the direction of the momentum k was taken along the quantization axis of the Ni ion. Such a simple treatment is reasonable since we are not aiming at absolute rate calculations but at computing the line shape. We recall that the above treatment yields an approximation to the *unrelaxed* spectrum. This means that we are ignoring the effects of the core-hole screening during its lifetime. Relaxation effects are discussed elsewhere,[31] but such complications do not seem necessary in the present instance.

II. RESULTS

In Fig. 3 AR-APECS spectra, that is Ni (*MVV*) Auger spectra measured in coincidence with Ni $3p$ photoelectrons collected at different angles, below T_N (upper panel) and above T_N, are presented. At room temperature, below T_N, a huge dichroism between AN geometry (green triangles with error bars) and NN geometry (red circles with error bars) makes several atomiclike multiplet terms distinguishable. At 420 K, above T_N, the contrast between AN and NN contributions disappears. The two AR-APECS measurements give, in the limit of the achieved statistics, the same line shape. A similar behavior, that is, the disappearance of the dichroic effect when

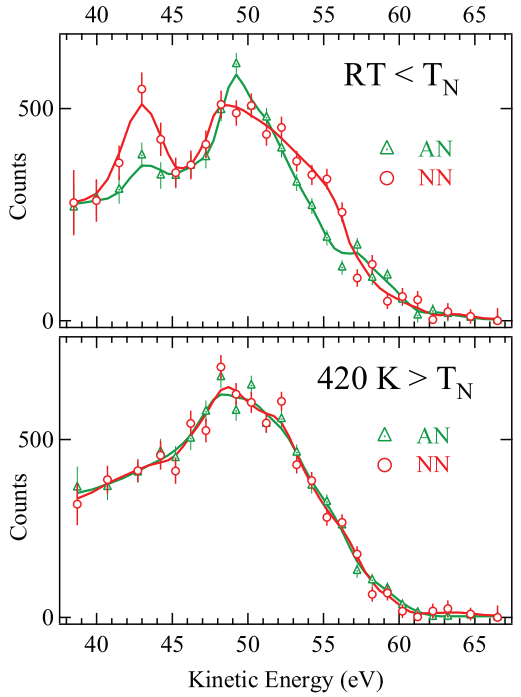

FIG. 3. (Color online) AR-APECS spectra of NiO/Ag in its AFM state at room temperature (upper panel) and its paramagnetic state at 420 K (lower panel). Green triangles and red circles with error bars show data collected in the AN and NN geometry, respectively. The solid lines joining coincidence data are spline fit acting as guides to the eyes.

crossing the antiferromagnetic-paramagnetic transition at T_N, has been found also in CoO/Ag(001).[18,19]

In order to correctly assign spin values to each of the multiplet terms singled out below T_N the theoretical model above presented has been used.

In Fig. 4 we display the XPS spectrum by Kowalczyk *et al.* (dashed line) as reported in Ref. 33 and the calculated LDOS (solid line) obtained by diagonalizing the Hamiltonian with two and three holes, and considering that a contribution of about 20% of the total intensity is due to photoemission from oxygen atoms.[33] The two-hole ground

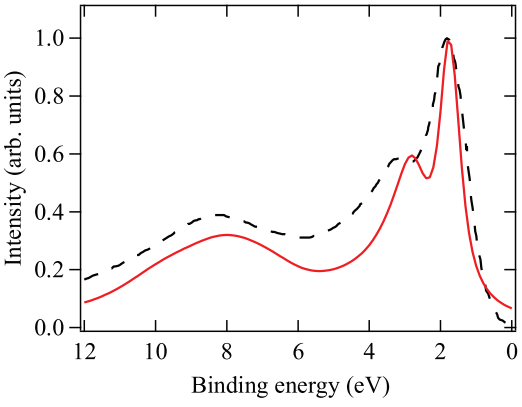

FIG. 4. (Color online) Comparison of experimental and calculated valence-band XPS profiles. Experimental spectrum from Ref. 33 (dashed line) and calculated (0.8 Ni + 0.2 O)-removal spectrum (solid line).

state (d^8 configuration) was taken to belong to maximum spin $S = 1$ in agreement with Hund's rule. After choosing the parameters that allow one to reproduce the main features of the experimental XPS spectrum, we estimated (in eV) $A = 3.1$, $\varepsilon_d(e_g) = -7.1$, $\varepsilon_d(t_{2g}) = -6.0$, $\varepsilon_p(e_g) = \varepsilon_p(t_{2g}) = 1.2$, $t_{pd}(e_{2g}2) = -1.6$, and $t_{pd}(t_{2g}) = -2.8$. As discussed in Ref. 33, the calculated spectrum has a broadening whose width increases (from 0.1 to 1 eV) with increasing binding energy in order to describe finite lifetime effects as well as the instrumental resolution. The intensity, width, and position of the three main peaks are very sensitive to the parameters and the agreement between theory and experiment is rather good, as all the main structures at 1.8 eV, 3.0 eV, and 8.3 eV are satisfactorily reproduced, both in energy and in relative amplitude. The same parameters are used to compute the Auger spectrum of the system.

The observation that in Fig. 3 a dichroic effect similar to the one seen in CoO is also visible in the AFM NiO film, motivated us to perform a calculation of the Auger line shape of NiO, in the same spirit of Ref. 19. For the Ni Auger spectrum, a Lorentzian of width 1 eV was convoluted to the function J to simulate lifetime and any other broadening effects. The NiO_6 cluster (10 orbitals) hosts four holes after the Auger decay and the rank of the full configuration interaction problem is $\binom{20}{4} = 4845$. Let H_{nm} denote the Hamiltonians with m spin-up and n spin-down holes; we cast H_{40}, H_{31}, and H_{22} in block form using the total spin S symmetry and found the eigenvalues and eigenvectors of the blocks. In particular, H_{22} has 210 quintets, 990 triplets, and 825 singlets, H_{31} has 210 quintets and 990 triplets, while H_{40} has only 210 quintets.

In Fig. 5 we compare the calculated spin-resolved Auger spectrum (lower panel) with the measured spectra (upper panel). The green, blue, and red lines show the contribution of

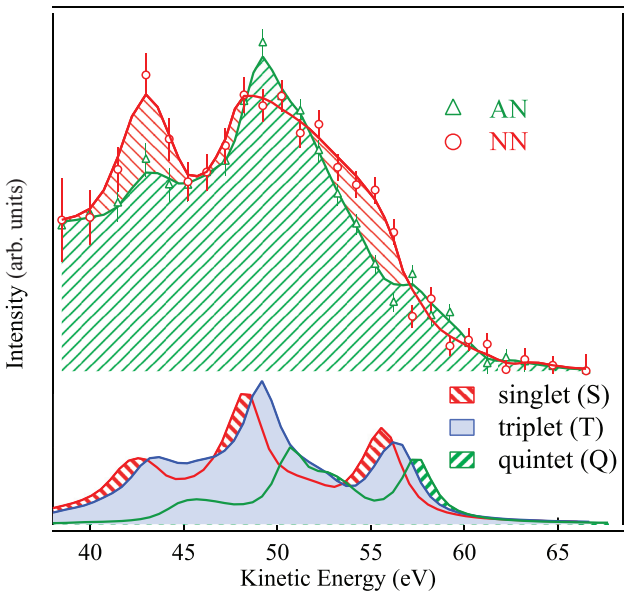

FIG. 5. (Color online) Comparison between experimental DEAR-APECS spectra of NiO (upper panel), for the AN (green triangles) and NN (red circles) geometries, and calculated unrelaxed spectrum (lower panel), resolved in spin for $S = 2$ (green, marked Q), $S = 1$ (blue, marked T), and $S = 0$ (red, marked S) components.

$S = 2$, $S = 1$, and $S = 0$, respectively, and will be referred to as quintet (Q), triplet (T), and singlet (S), respectively.

As in the case of CoO, once theoretical and experimental spectra are aligned, the whole pattern of peaks agrees with the experiment, allowing for an unambiguous assignment of all the main features. A clear feature at 57.5 eV in the AN curve coincides with structures in the Q and T curves in that energy region, while the feature appearing at 56 eV in the NN curve may be assigned to the corresponding maximum in the S curve. The maximum at 50 eV followed by a shoulder at 52 eV of AN correspond to T and Q peaks, respectively, while the broader maximum of NN corresponds to the S and T maxima. The AN maximum at 43 eV corresponds to a peak in the T curve while the S maximum at a slightly lower kinetic energy should account for a more distinct peak in the same region for the NN configuration. The analysis is more difficult than in the CoO case because the different spins are not so nicely separated in NiO, but from the above comparisons, it results that the NN curve is mainly a combination of S and T while AN is mainly T and Q: The quintet gives a minor contribution to both experimental profiles and the main change when going from the AN to the NN configuration is an increase of the singlet contribution at the expenses of the triplet one.

III. DISCUSSION

The mechanism for the occurrence of the DEAR-APECS in the present case of transition-metal oxides AFM is somehow different to what has been observed in metallic FM. In that case the DEAR-APECS has been explained[16] in terms of different total spin of the two-hole final state when combining in a band-like fashion (self-convolutions of the density of states) majority and minority electrons contributions to the Auger decay. Majority-majority, minority-minority, and majority-minority self-convolutions result to be slightly shifted in energy due to the band splitting. Only for an ultrathin film an enhanced energy shift, according to the Cini-Sawatzky approach, has been measured for the majority-majority contribution revealing a stronger degree of localization in the polarized majority subband only.[17] The Cini-Sawatzky approach, indeed, allows one to describe electronic correlation effects in the Auger line shape and an energy shift from the Fermi level toward higher binding energies (i.e., lower kinetic energies) is expected when going from bandlike to atomiclike behaviors. As in our case there is no evidence for an energy shift of the Auger line when crossing T_N; the disappearance of the DEAR-APECS effect above T_N cannot be explained in terms of a change from an atomiclike to a bandlike behavior or, in other words, invoking a different degree of electron-electron correlation.

On the other hand, the results here presented indicate a close similarity between the DEAR-APECS spectra of NiO and CoO,[18] the only difference being a higher propensity of CoO to satisfy the Hund's rule, with clearer evidence of low-spin intensity in contributing to the higher binding energies part of the Auger spectrum and, vice versa, high-spin intensity getting closer to the Fermi edge. In NiO, instead, the three singlet, triplet, and quintet contributions are shifted in energy according to the Hund's rule, but their individual energy distributions are quite similar and do not enhance such a behavior as in CoO. Such a similar behavior, previously found in CoO and here confirmed for NiO, put in evidence a general behavior of the local electronic structure when crossing the magnetic transition, at least for metal oxide systems. While below T_N the DEAR-APECS allows one to disentangle high-spin and low-spin multiplet terms contributing to the total Auger intensity, above T_N, AR-APECS spin selectivity is lost and identical, more featureless, Auger line shapes are obtained in the two different geometries. In the CoO case, two contributing effects have been taken into account: (1) the presence of magnetic moments affecting the DEAR-APECS effect via matrix elements,[38] and (2) changes in the screening channels at the two temperatures.[18] In both cases, the local character of the effects has been emphasized, which is still valid for NiO.

At the present level of understanding we limit ourselves in determining where, from the experimental point of view, the loss of spin selectivity could originate from, when referring to extra particles (like screening electrons) participating in the Auger decay. We start from the essential assessment that high-spin and low-spin multiplet structures distinguished below T_N are no more disentangled by AR-APECS above T_N. In principle, this doesn't mean that above T_N a multiplet structure has to be excluded in the Auger final state; it simply tells us that the angle-resolved coincident detection of two electrons (the Auger electron together with its parent photoelectron) no longer allows for achieving the final state spin selectivity. In order to understand what such a claim entails, we should go back to the difference between conventional AES, where spin selectivity is absent, and AR-APECS where the intensity of multiplet terms having specific spin values, can be enhanced or suppressed. The core-valence-valence Auger matrix elements involve a two-body operator (the Coulomb interaction) and create two holes in the valence band. In conventional AES we detect only one (the Auger electron) of the two electrons leaving the valence band, the other one going to fill the core hole previously created by the photoionization. In this circumstance, in which we have no information on the latter electron, we cannot access the spin value of the two-hole final state and, if we want to describe the AES line shape, we have to integrate over all the possible states of the "nondetected electron," that is, over all the intermediated core-hole states. In APECS, on the other hand, by detecting in time coincidence the parent photoelectron leaving the core hole, it is as if the second electron leaving the valence band were detected; in fact, Auger decay and photoemission selection rules make the relevant quantum numbers connected between the valence electron and the core hole and between the core hole and the photoelectron, respectively. In this way the measure can access the spin value of the electron leaving the valence band and filling the core hole and such a "double detection" activates the selectivity on the spin value of the multiplet terms in the Auger final state, or, in other words, coincidence measurement of the two electrons removes a sum over unknown (not detected) states, the averaging of which obscures the fine structures in the Auger line shape. Finally, the detection of a single electron in AES makes it not able to get details (spin value) on the two-hole final state while in principle the "double detection" in AR-APECS can; similarly, the same "double detection" in AR-APECS above T_N may no longer be able to get spin selectivity if a new, third particle (or event) participates in the decay. This makes the total spin not accessible with "only"

two electrons measured, and a new sum over unknown (not detected) states obscures structures in the final state.

IV. CONCLUSIONS

The DEAR-APECS is now a well-established effect and consists of a redistribution of the Auger intensity between high-spin and low-spin multiplet components in the final state when comparing emission geometries having different alignment with respect to the photon linear polarization. The effect, in transition-metal oxides, occurs in the AFM phase and disappears in the paramagnetic phase. The good agreement with the calculated positions of these structures permits an unambiguous assignment of atomiclike multiplet terms as main structures in the Auger profile below T_N. This opens up the possibility of monitoring magnetic transitions from a localized perspective, without having to rely on crystal periodicity or bulk thermodynamic measurements. On the other hand we need a unified theory of the mechanism responsible for the DEAR-APECS capable of explaining specific behaviors in different magnetic systems, in particular when crossing transition temperatures.

ACKNOWLEDGMENTS

The experiments reported in this paper have been possible thanks to the dedicated support received by the scientists in charge of the ALOISA beamline at the ELETTRA synchrotron radiation facility. We gratefully acknowledge financial support from MIUR PRIN 2008 Contract No. 2008AKZSXY.

*Present address: MPI-Halle Exp. Dept. I, Weinberg 2, 06120 Halle (Saale), Germany.

[1] J. C. Slater, Phys. Rev. B **82**, 538 (1951).
[2] E. P. Wohlfarth, Rev. Mod. Phys. **25**, 211 (1953).
[3] M. A. Mook, J. W. Lynn, and R. M. Nicklow, Phys. Rev. Lett. **30**, 556 (1973).
[4] J. Kirschner and E. Langhenbach, Solid. State Commun. **66**, 761 (1988).
[5] B. Sinkovic, L. H. Tjeng, N. B. Brookes, J. B. Goedkoop, R. Hesper, E. Pellegrin, F. M. F. de Groot, S. Altieri, S. L. Hulbert, E. Shekel, and G. A. Sawatzky, Phys. Rev. Lett. **79**, 3510 (1997).
[6] F. Offi, W. Kuch, and J. Kirschner, Phys. Rev. B **66**, 064419 (2002).
[7] K. Lenz, S. Zander, and W. Kuch, Phys. Rev. Lett. **98**, 237201 (2007).
[8] G. Ghiringhelli, L. H. Tjeng, A. Tanaka, O. Tjernberg, T. Mizokawa, J. L. de Boer, and N. B. Brookes, Phys. Rev. B **66**, 075101 (2002).
[9] I. D. Hughes, M. Däne, A. Ernst, W. Hergert, M. Lüders, J. B. Staunton, Z. Szotek, and W. M. Temmerman, New J. Phys. **10**, 063010 (2008).
[10] M. Pickel, A. B. Schmidt, M. Weinelt, and M. Donath, Phys. Rev. Lett. **104**, 237204 (2010).
[11] S. Sanna, P. Carretta, P. Bonfà, G. Prando, G. Allodi, R. De Renzi, T. Shiroka, G. Lamura, A. Martinelli, and M. Putti, Phys. Rev. Lett. **107**, 227003 (2011).
[12] H. W. Haak, G. A. Sawatzky, and T. D. Thomas, Phys. Rev. Lett. **41**, 1825 (1978).
[13] R. Gotter, A. Ruocco, M. T. Butterfield, S. Iacobucci, G. Stefani, and R. A. Bartynski, Phys. Rev. B **67**, 033303 (2003).
[14] G. Stefani, R. Gotter, A. Ruocco, F. Offi, F. Da Pieve, S. Iacobucci, A. Morgante, A. Verdini, A. Liscio, H. Yao, and R. A. Bartynski, J. Electron Spectrosc. Relat. Phenom. **141**, 149 (2004).
[15] R. Gotter, F. Da Pieve, A. Ruocco, F. Offi, G. Stefani, and R. A. Bartynski, Phys. Rev. B **72**, 235409 (2005).
[16] R. Gotter, F. Offi, F. Da Pieve, A. Ruocco, G. Stefani, S. Ugenti, M. I. Trioni, and R. A. Bartynski, J. Electron Spectrosc. Relat. Phenom. **161**, 128 (2007).
[17] R. Gotter, G. Fratesi, R. A. Bartynski, F. DaPieve, F. Offi, A. Ruocco, S. Ugenti, M. I. Trioni, G. P. Brivio, and G. Stefani, Phys. Rev. Lett. **109**, 126401 (2012).
[18] R. Gotter, F. Offi, A. Ruocco, F. Da Pieve, R. A. Bartynski, M. Cini, and G. Stefani, Europhys. Lett. **94**, 37008 (2011).
[19] M. Cini, E. Perfetto, R. Gotter, F. Offi, A. Ruocco, and G. Stefani, Phys. Rev. Lett. **107**, 217602 (2011).
[20] M. Caffio, B. Cortigiani, G. Rovida, A. Atrei, and C. Giovanardi, J. Phys. Chem. B **108**, 9919 (2004).
[21] M. Caffio, A. Atrei, B. Cortigiani, and G. Rovida, J. Phys.: Condens. Matter **18**, 2379 (2006).
[22] C. S. Fadley, in *Electron Spectroscopy: Theory, Techniques and Applications*, edited by C. R. Brundle and A. D. Baker (Pergamon Press, Oxford, 1978), Chap. 3, Sec. F, pp. 72–73.
[23] S. Altieri, M. Finazzi, H. H. Hsieh, H.-J. Lin, C. T. Chen, T. Hibma, S. Valeri, and G. A. Sawatzky, Phys. Rev. Lett. **91**, 137201 (2003).
[24] D. Alders, L. H. Tjeng, F. C. Voogt, T. Hibma, G. A. Sawatzky, C. T. Chen, J. Vogel, M. Sacchi, and S. Iacobucci, Phys. Rev. B **57**, 11623 (1998).
[25] M. W. Haverkort, S. I. Csiszar, Z. Hu, S. Altieri, A. Tanaka, H. H. Hsieh, H.-J. Lin, C. T. Chen, T. Hibma, and L. H. Tjeng, Phys. Rev. B **69**, 020408 (2004).
[26] E. Arenholz, G. van der Laan, R. V. Chopdekar, and Y. Suzuki, Phys. Rev. Lett. **98**, 197201 (2007).
[27] R. Gotter, A. Ruocco, A. Morgante, D. Cvetko, L. Floreano, F. Tommasini, and G. Stefani, Nucl. Instrum. Methods Phys. Res. A **467-468**, 1468 (2001).
[28] R. Gotter, F. Da Pieve, F. Offi, A. Ruocco, A. Verdini, H. Yao, R. A. Bartynski, and G. Stefani, Phys. Rev. B **79**, 075108 (2009).
[29] M. Cini, Solid State Commun. **24**, 681 (1977).
[30] G. A. Sawatzky, Phys. Rev. Lett. **39**, 504 (1977).
[31] M. Cini and V. Drchal, J. Electron Spectrosc. Relat. Phenom. **72**, 151 (1995).
[32] O. Gunnarsson and K. Schönhammer, Phys. Rev. B **26**, 2765 (1982).
[33] A. Fujimori and F. Minami, Phys. Rev. B **30**, 957 (1984).
[34] E. Clementi and C. Roetti, At. Data Nucl. Data Tables **14**, 177 (1974).
[35] J. Zaanen, G. A. Sawatzky, and J. W. Allen, Phys. Rev. Lett. **55**, 418 (1985).
[36] J. C. Slater and G. F. Koster, Phys. Rev. **94**, 1498 (1954).
[37] Giulio Racah, Phys. Rev. **62**, 438 (1942).
[38] F. Da Pieve, S. Fritzsche, G. Stefani, and N. M. Kabachnik, J. Phys. B: At. Mol. Opt. Phys. **40**, 329 (2007).